

Van der Westhuizen, M. & Abebe, A. (2026). Unified dark fluid models of interacting dark energy. In Abebe, A. & Paliathanasis, A. (eds), *Proceedings of the South African Gravity Society Conference 2025 (SAGS2025)*. Potchefstroom: Axiom Academic Publishers, pp. 62 - 80.

CHAPTER 6

Unified dark fluid models of interacting dark energy

Marcel van der Westhuizen and Amare Abebe

Abstract

Interacting dark energy (IDE) models in which non-gravitational interactions occur between dark matter and dark energy are popular candidates for addressing various cosmological tensions, but these models may suffer from negative energy densities and divergences in the effective equations of state near phantom-divide crossing. Here, we present an equivalent Unified Dark Fluid (UDF) description of a group of eight interacting dark energy models, which can avoid these pathologies. We present analytical solutions for the total UDF density $\rho_{\rm D}$ and the effective UDF equation of state $w_{\rm D}^{\rm eff}$, and show that both negative energies and divergences are avoided, which normally arise in the two-fluid decomposition. As a case study, we show that one of the IDE models is equivalent, at the background level, to a Generalized Chaplygin Gas (GCG) fluid under a new transformation. We then use recent observational constraints on the IDE models to infer implications for their unified dark fluid description. This study demonstrates that certain pathologies of interacting dark energy models arise from the two-fluid decomposition rather than from the background cosmology itself.

Keywords: Interacting dark energy; unified dark fluid; Chaplygin gas; phantom divide

Unified Dark Fluid Models of Interacting Dark Energy

Marcel van der Westhuizen[1] and Amare Abebe[1,2]

[1]Centre for Space Research, North-West University, Potchefstroom 2520, South Africa
[2]National Institute for Theoretical and Computational Sciences (NITheCS), South Africa
[1]E-mail: marcelvdw007@gmail.com

Abstract

Interacting dark energy (IDE) models in which non-gravitational interactions occur between dark matter and dark energy are popular candidates for addressing various cosmological tensions, but these models may suffer from negative energy densities and divergences in the effective equations of state near phantom-divide crossing. Here, we present an equivalent Unified Dark Fluid (UDF) description of a group of eight interacting dark energy models, which can avoid these pathologies. We present analytical solutions for the total UDF density $\rho_{\rm D}$ and the effective UDF equation of state $w_{\rm D}^{\rm eff}$, and show that both negative energies and divergences are avoided, which normally arise in the two-fluid decomposition. As a case study, we show that one of the IDE models is equivalent, at the background level, to a Generalized Chaplygin Gas (GCG) fluid under a new transformation. We then use recent observational constraints on the IDE models to infer implications for their unified dark fluid description. This study demonstrates that certain pathologies of interacting dark energy models arise from the two-fluid decomposition rather than from the background cosmology itself.

1 Introduction

Simple models where dark matter and dark energy are allowed to interact in a non-gravitational manner, known as Interacting Dark Energy (IDE) models, have been popular candidates in recent years for addressing growing tensions in the standard ΛCDM model of cosmology. These include the recent indications of evolving dark energy from DESI analyses [1, 2], the persistent Hubble and S_8 tensions [3–5], as well as older theoretical concerns such as the coincidence problem [6–8]. Although dark sector interactions have at various times been proposed to address or solve each of these issues [9–17], these models face their own challenges. Among other problems, these models often lack microphysical descriptions, and certain parts of the parameter space of IDE models tend to suffer from instabilities [18–20] and negative energy densities in the dark sectors [21–25], accompanied by divergences in the effective equations of state for dark matter and dark energy.

These problems are active areas of research, as recent examples of IDE models with microphysical descriptions have been suggested in [16, 26–28], while developments with regard to IDE perturbations and avoiding instabilities are given in [29–31]. The negative energy issues are less discussed in the literature, but of equal importance. Of particular concern is that negative energies tend to show up when energy flows from dark matter to dark energy, the direction of energy transfer that may alleviate the Hubble tension [15, 32]. This issue has motivated some authors to restrict the parameter space to regions where the energy densities remain positive [14]; or to limit the accessible parameter space to cases corresponding to energy flow from dark energy to dark matter (avoiding negative energies), corresponding to the $+iw$CDM regime outlined in [25]. This sets artificial constraints when performing Markov Chain Monte Carlo (MCMC) analysis, reducing the available parameter space and thus the potential of these models to solve problems in cosmology. Otherwise, the entire parameter space may be utilised when performing observational constraints, often giving posteriors corresponding to energy flow from dark matter to dark energy, and hence negative energies [33]. In this latter case, one may be sceptical about the results, as they may point to unphysical scenarios.

This is still an open question, as some researchers do not only allow for negative dark sector energies, but actively use them to address problems in cosmology. Examples of sign-switching or negative dark energy models are found in [34–41], while negative dark matter (or other negative mass) models are explored in [42–46]. Other approaches propose that the IDE kernels should not be extended beyond their domain of applicability, i.e. to the distant future or to very early times (high redshift), thus avoiding the problems associated with these regions. An example would be modelling the interaction kernel as something which only switches on at late times and low redshift [47]. In

either case, one has to be careful about how negative energy can violate the energy conditions of general relativity [48, 49]. In this paper, we look at a possible approach to rethinking the issue of negative energy densities.

The negative energy density problem in IDE models arises from the way the dark sector is partitioned in equation (1), such that energy transfer may continue even when the densities are zero, thus causing the individual dark matter or dark energy components to become negative [23–25]. We may note that the total dark sector can still remain positive in these cases. Furthermore, at the background level, the expansion of the universe is only dependent on the total energy density of the universe and not the density of the individual components. This implies that it is difficult to distinguish the effects of dark sector interactions from other models such as dynamical dark energy, unified dark sector models, modified gravity, Chevallier–Polarski–Linder (CPL) parametrization, etc. This is a manifestation of the so-called "dark degeneracy" [50–53]. Given these considerations, it is natural to consider a unified dark fluid (UDF) interpretation of interacting dark energy. Some recent work on unified dark fluid models can be found in [54]. The aim is to avoid negative energy densities in the total dark sector while preserving the same background expansion history, thereby allowing a wider region of parameter space to remain physically viable and enhancing the ability of IDE models to address cosmological tensions such as the Hubble tension.

In this work we show that a broad class of interacting dark energy models admits an equivalent UDF description at the background level. In this formulation the total dark sector energy density remains positive for all finite cosmic times, even in cases where the individual dark matter and dark energy components become negative in the standard two–fluid decomposition. The equivalence preserves the background dynamics of the original IDE models, and therefore represents a reinterpretation rather than a modification of the cosmology. We emphasize that this equivalence holds only at the level of the background expansion; perturbations will in general distinguish between the interacting and unified descriptions.

This work is structured as follows. In section 2, we show how IDE models may be converted into UDF descriptions that always have positive energy densities, while maintaining the same background dynamics. This is then applied in section 3, where we convert eight phenomenological IDE models into UDF descriptions providing new analytic equations for the total dark fluid $\rho_{\rm D}(z)$, the effective unified dark fluid equation of state $w_{\rm D}^{\rm eff}(z)$. In subsection 3.9, we plot the evolution $\rho_{\rm D}(z)$ and $w_{\rm D}^{\rm eff}(z)$ to show how this interpretation avoids the negative energy problem and the above mentioned divergences in the equations of state. To make the connection between IDE models and a UDF description stronger, we show in section 4 how one specific IDE kernel can be reinterpreted as a Generalized Chaplygin Gas (GCG) fluid under a new transformation (29) and show equivalence between the models. In section 5, we mention some implications when combining our UDF framework with recent observational constraints obtained from late-time data on the same interaction kernels studied here [33]. Finally, in section 6, we draw conclusions and discuss future work.

This work presents a proof-of-concept demonstration that interacting dark energy models can be consistently reinterpreted within a unified dark fluid framework at the background level. A more complete study would require considering perturbations as well, in which there is a definite difference between the dark matter and dark energy components, thus breaking the degeneracy. This may be considered in future work, but for now we point the curious reader to [54, 55], and our brief discussion in Appendix A: A brief note on perturbations in UDF and IDE models.

2 Unified Dark Fluid description of IDE models

Interacting dark energy models are usually described with the two coupled conservation equations of dark matter and dark energy, which conserve the total dark sector, but not the individual species:

$$\dot{\rho}_{\rm dm} + 3H\rho_{\rm dm} = Q \ , \qquad \dot{\rho}_{\rm de} + 3H(1+w)\rho_{\rm de} = -Q \ , \tag{1}$$

where $\rho_{\rm dm}$ and $\rho_{\rm de}$ are the energy densities of dark matter and dark energy, w is the dark energy equation of state, H is the Hubble parameter and Q determines how the energy is transferred between the fluids. The negative energies mentioned above arise from the fact that often $Q \neq 0$ when either $\rho_{\rm dm} = 0$ or $\rho_{\rm de} = 0$, allowing the energy densities to cross into negative values. This may be avoided with a single fluid description, which is obtained by adding the two conservation equations together to give:

$$\dot{\rho}_{\rm D} + 3H\rho_{\rm D}[1 + w_{\rm D}^{\rm eff}(z)] = 0 \ , \tag{2}$$

where $\rho_{\rm D}$ is the total dark sector density given in (3) and $w_{\rm D}^{\rm eff}(z)$ is the effective dynamical equation of state of the single fluid. The energy density $\rho_{\rm D}$ and pressure $p_{\rm D}$ of the total fluid is related and given by:

$$\rho_{\rm D} = \rho_{\rm dm} + \rho_{\rm de} \quad ; \quad p_{\rm D} = p_{\rm dm} + p_{\rm de} = w\rho_{\rm de}, \tag{3}$$

where we have assumed dark matter to be inherently pressureless $p_{\rm dm} = 0$, and w is the equation of state of the dark energy component. The effective dynamical equation of state of the single fluid is obtained from (3) as:

$$w_{\rm D}^{\rm eff}(z) = \frac{p_{\rm D}}{\rho_{\rm D}} = \frac{w\rho_{\rm de}(z)}{\rho_{\rm dm}(z) + \rho_{\rm de}(z)} = \frac{w}{1 + r(z)}. \tag{4}$$

Here we have defined $r(z) \equiv \rho_{\rm dm}(z)/\rho_{\rm de}(z)$, such that the present ratio is $r_0 = r(0) = \rho_{\rm (dm,0)}/\rho_{\rm (de,0)}$. In the two fluid description, negative dark matter and dark energy densities, accompanied by divergent effective equations of state for dark matter $w_{\rm dm}^{\rm eff}$ and $w_{\rm de}^{\rm eff}$, often show up when energy flows from dark matter to dark energy, as seen in Figure 1 and [23, 24]. Intuitively, we can note from (2) that when $\rho_{\rm D} = 0$, the derivative vanishes, i.e., $\dot{\rho}_{\rm D} = 0$. This implies that once the total dark sector starts positive $\rho_{\rm (D,0)} > 0$, the total fluid cannot cross into negative values (although the individual dark matter and dark energy components can). More formally, since $w_{\rm D}^{\rm eff}(z)$ is undefined at $\rho_{\rm D} = 0$, we may instead note that (2) is a linear first-order ordinary differential equation with the following solution:

$$\rho_{\rm D}(a) = \rho_{\rm (D,0)} \exp\left[-3\int_{a_0}^{a} \frac{1 + w_{\rm D}^{\rm eff}(a)}{a}\, da\right]. \tag{5}$$

The exponential factor is always positive whenever the integral is finite, implying that if $\rho_{\rm D,0} > 0$ then $\rho_{\rm D}(a) > 0$ for all finite a. Possible divergences of $w_{\rm D}^{\rm eff}$ can only drive $\rho_{\rm D}$ to 0 or ∞ (depending on the sign of the integral), but do not produce a crossing into negative values. One exception to this interpretation occurs in the strongly interacting regime, where the total dark sector may cross $\rho_{\rm D} = 0$. In this case $w_{\rm D}^{\rm eff}$ in (2) and (4) is no longer well defined, so the evolution lies outside the regular UDF branch assumed in (5). This is discussed in Appendix B: Domain of validity of the UDF description.

3 Analytical solutions for UDF description of IDE fluids

For this study, we will only consider the phenomenological IDE models that have analytical solutions for $\rho_{\rm dm}$ and $\rho_{\rm de}$ as found in [25]. For other models, see the IDE review papers [56, 57]. We propose the following general interaction function Q, from which any of the eight interactions that we consider can be obtained after specifying α and β and the two coupling constants $\delta_{\rm dm}$ and $\delta_{\rm de}$:

$$Q = 3H\left[\frac{\delta_{\rm dm}\rho_{\rm dm}^{\alpha}\rho_{\rm de}^{\beta} + \delta_{\rm de}\rho_{\rm dm}^{\beta}\rho_{\rm de}^{\alpha}}{(\rho_{\rm dm} + \rho_{\rm de})^{\alpha+\beta-1}}\right] \tag{6}$$

Using (6), we can obtain each model for the special cases shown in Table 1. Here $\delta_{\rm dm}$ and $\delta_{\rm de}$ tell us if the coupling is dependent on either dark matter or dark energy, while α tells us if the coupling to that fluid is linear ($\alpha = 1$) or non-linear ($\alpha = 2$), while β is specially reserved for couplings which depend on the product of both fluids ($\beta = 1$), and hence always avoid negative energies. To obtain the analytical solutions for $\rho_{\rm D}(z)$ $w_{\rm D}^{\rm eff}(z)$ given in section 3, we will substitute the relevant expressions found in [23, 24] into (3) and (4), and do the necessary simplification.

Table 1: Special cases of (6) which lead to familiar linear and non-linear interaction functions.

Interaction Q	α	β	$\delta_{\rm dm}$	$\delta_{\rm de}$
$3H(\delta_{\rm dm}\rho_{\rm dm} + \delta_{\rm de}\rho_{\rm de})$	1	0	$\delta_{\rm dm}$	$\delta_{\rm de}$
$3H\delta(\rho_{\rm dm} + \rho_{\rm de})$	1	0	δ	δ
$3H\delta(\rho_{\rm dm} - \rho_{\rm de})$	1	0	δ	$-\delta$
$3H\delta\rho_{\rm dm}$	1	0	δ	0
$3H\delta\rho_{\rm de}$	1	0	0	δ
$3H\delta\left(\frac{\rho_{\rm dm}\rho_{\rm de}}{\rho_{\rm dm}+\rho_{\rm de}}\right)$	1	1	δ	0
$3H\delta\left(\frac{\rho_{\rm dm}^2}{\rho_{\rm dm}+\rho_{\rm de}}\right)$	2	0	δ	0
$3H\delta\left(\frac{\rho_{\rm de}^2}{\rho_{\rm dm}+\rho_{\rm de}}\right)$	2	0	0	δ

3.1 Linear IDE model 1: $Q = 3H(\delta_{\mathbf{dm}}\rho_{\mathbf{dm}} + \delta_{\mathbf{de}}\rho_{\mathbf{de}})$

This IDE model may experience $\rho_{\rm de} < 0$ alongside $w_{\rm de}^{\rm eff} = \pm\infty$ in the past if $\delta_{\rm dm} < 0$, and $\rho_{\rm dm} < 0$ alongside $w_{\rm dm}^{\rm eff} = \pm\infty$ in the future if $\delta_{\rm de} < 0$, as shown in [23].

The energy density of the UDF is obtained by substituting equations (5.1) and (5.2) from [23] into (3) to obtain:

$$\begin{aligned}\rho_{\rm D}(z) = &-\frac{1}{2\Delta}\Big[\rho_{\rm (de,0)}\Big(\delta_{\rm dm} - \delta_{\rm de} + w - \Delta\Big) + \rho_{\rm (dm,0)}\Big(\delta_{\rm dm} - \delta_{\rm de} - w - \Delta\Big)\Big](1+z)^{-\frac{3}{2}\left(\delta_{\rm dm}-\delta_{\rm de}-w-2+\Delta\right)} \\ &+\frac{1}{2\Delta}\Big[\rho_{\rm (de,0)}\Big(\delta_{\rm dm} - \delta_{\rm de} + w + \Delta\Big) + \rho_{\rm (dm,0)}\Big(\delta_{\rm dm} - \delta_{\rm de} - w + \Delta\Big)\Big](1+z)^{-\frac{3}{2}\left(\delta_{\rm dm}-\delta_{\rm de}-w-2-\Delta\right)}.\end{aligned} \tag{7}$$

The equation of state for the UDF is obtained by substituting equations (5.1) and (5.2) from [23] into (4):

$$\begin{aligned}w_{\rm D}^{\rm eff}(z) = &\Big\{ -(\delta_{\rm dm} - \delta_{\rm de} - w + \Delta)\left[\Omega_{\rm (de,0)}(\delta_{\rm dm} - \delta_{\rm de} + w - \Delta) + \Omega_{\rm (dm,0)}(\delta_{\rm dm} - \delta_{\rm de} - w - \Delta)\right](1+z)^{-3\Delta} \\ &+(\delta_{\rm dm} - \delta_{\rm de} - w - \Delta)\left[\Omega_{\rm (de,0)}(\delta_{\rm dm} - \delta_{\rm de} + w + \Delta) + \Omega_{\rm (dm,0)}(\delta_{\rm dm} - \delta_{\rm de} - w + \Delta)\right]\Big\} \\ &\times\frac{1}{2}\Big\{\left[\Omega_{\rm (de,0)}(\Delta + \delta_{\rm de} - \delta_{\rm dm} - w) + \Omega_{\rm (dm,0)}(\Delta + \delta_{\rm de} - \delta_{\rm dm} + w)\right](1+z)^{-3\Delta} \\ &+\left[\Omega_{\rm (de,0)}(\Delta - \delta_{\rm de} + \delta_{\rm dm} + w) + \Omega_{\rm (dm,0)}(\Delta - \delta_{\rm de} + \delta_{\rm dm} - w)\right]\Big\}^{-1},\end{aligned} \tag{8}$$

with the determinant in both cases $\Delta = \sqrt{\left(\delta_{\rm dm} + \delta_{\rm de} + w\right)^2 - 4\,\delta_{\rm de}\delta_{\rm dm}}$.

3.2 Linear IDE model 2: $Q = 3H\delta(\rho_{\mathbf{dm}} + \rho_{\mathbf{de}})$

For this IDE model, if energy transfers from dark matter to dark energy ($\delta < 0$), the model experiences both $\rho_{\rm de} < 0$ and $\rho_{\rm dm} < 0$ (alongside $w_{\rm de}^{\rm eff} = \pm\infty$ and $w_{\rm dm}^{\rm eff} = \pm\infty$) in the past and future respectively, as shown in [23] and seen in Figure 1.

Substituting equations (5.17) and (5.18) from [23] into (3) yields:

$$\begin{aligned}\rho_{\rm D}(z) = &-\frac{1}{2\Delta}\Big[\rho_{\rm (de,0)}(w - \Delta) + \rho_{\rm (dm,0)}(-w - \Delta)\Big](1+z)^{-\frac{3}{2}(-w-2+\Delta)} \\ &+\frac{1}{2\Delta}\Big[\rho_{\rm (de,0)}(w + \Delta) + \rho_{\rm (dm,0)}(-w + \Delta)\Big](1+z)^{-\frac{3}{2}(-w-2-\Delta)}.\end{aligned} \tag{9}$$

Substituting equations (5.17) and (5.18) from [23] into (4) gives:

$$\begin{aligned}w_{\rm D}^{\rm eff}(z) = &\Big\{ -(-w + \Delta)\left[\Omega_{\rm (de,0)}(w - \Delta) + \Omega_{\rm (dm,0)}(-w - \Delta)\right](1+z)^{-3\Delta} \\ &+(-w - \Delta)\left[\Omega_{\rm (de,0)}(w + \Delta) + \Omega_{\rm (dm,0)}(-w + \Delta)\right]\Big\} \\ &\times\frac{1}{2}\Big\{\left[\Omega_{\rm (de,0)}(\Delta - w) + \Omega_{\rm (dm,0)}(\Delta + w)\right](1+z)^{-3\Delta} + \left[\Omega_{\rm (de,0)}(\Delta + w) + \Omega_{\rm (dm,0)}(\Delta - w)\right]\Big\}^{-1}.\end{aligned} \tag{10}$$

with the determinant in both cases $\Delta = \sqrt{w\,(4\delta + w)}$.

3.3 Linear IDE model 3: $Q = 3H\delta(\rho_{\mathbf{dm}} - \rho_{\mathbf{de}})$

This is a sign changing interaction, with the sign of δ determining the initial direction of energy transfer. When $\delta < 0$, the model may experience $\rho_{\rm de} < 0$ alongside $w_{\rm de}^{\rm eff} = \pm\infty$ in the past. If $\delta > 0$, then $\rho_{\rm dm} < 0$ alongside $w_{\rm dm}^{\rm eff} = \pm\infty$ in the future, as shown in [23] and seen in Figure 1.

Substituting equations (5.32) and (5.33) from [23] into (3) yields:

$$\begin{aligned}\rho_{\rm D}(z) = &-\frac{1}{2\Delta}\Big[\rho_{\rm (de,0)}(2\delta + w - \Delta) + \rho_{\rm (dm,0)}(2\delta - w - \Delta)\Big](1+z)^{-\frac{3}{2}(2\delta-w-2+\Delta)} \\ &+\frac{1}{2\Delta}\Big[\rho_{\rm (de,0)}(2\delta + w + \Delta) + \rho_{\rm (dm,0)}(2\delta - w + \Delta)\Big](1+z)^{-\frac{3}{2}(2\delta-w-2-\Delta)}.\end{aligned} \tag{11}$$

Substituting equations (5.32) and (5.33) from [23] into (4) gives:

$$\begin{aligned} w_{\rm D}^{\rm eff}(z) = \Big\{ &- (2\delta - w + \Delta)\left[\Omega_{\rm (de,0)}\,(2\delta + w - \Delta) + \Omega_{\rm (dm,0)}\,(2\delta - w - \Delta)\right](1+z)^{-3\Delta} \\ &+ (2\delta - w - \Delta)\left[\Omega_{\rm (de,0)}\,(2\delta + w + \Delta) + \Omega_{\rm (dm,0)}\,(2\delta - w + \Delta)\right]\Big\} \\ \times\frac{1}{2}\Big\{ &\left[\Omega_{\rm (de,0)}\,(\Delta - 2\delta + w) + \Omega_{\rm (dm,0)}\,(\Delta - 2\delta - w)\right](1+z)^{-3\Delta} \\ &+ \left[\Omega_{\rm (de,0)}\,(\Delta + 2\delta + w) + \Omega_{\rm (dm,0)}\,(\Delta + 2\delta - w)\right]\Big\}^{-1}. \end{aligned} \tag{12}$$

with the determinant in both cases $\Delta = \sqrt{4\delta^2 + w^2}$.

3.4 Linear IDE model 4: $Q = 3H\delta\rho_{\rm dm}$

When energy flows from dark matter to dark energy ($\delta < 0$), the model may experience $\rho_{\rm de} < 0$ alongside $w_{\rm de}^{\rm eff} = \pm\infty$ in the past, as shown in [23] and seen in Figure 1.

Substituting equations (5.47) and (5.48) from [23] into (3) gives:

$$\rho_{\rm D}(z) = \rho_{\rm (dm,0)}(1+z)^{3(1-\delta)} + \left(\rho_{\rm (de,0)} + \rho_{\rm (dm,0)}\left(\frac{\delta}{\delta + w}\right)\left[1 - (1+z)^{-3(\delta+w)}\right]\right)(1+z)^{3(w+1)}. \tag{13}$$

Substituting equations (5.47) and (5.48) from [23] into (4) yields:

$$w_{\rm D}^{\rm eff}(z) = w\,\frac{\delta\,\Omega_{\rm (dm,0)} - \Big[\Omega_{\rm (de,0)}(\delta + w) + \Omega_{\rm (dm,0)}\delta\Big](1+z)^{3(\delta+w)}}{\Big[\Omega_{\rm (de,0)}(\delta + w) + \Omega_{\rm (dm,0)}\delta\Big](1+z)^{3(\delta+w)} + w\,\Omega_{\rm (dm,0)}}. \tag{14}$$

3.5 Linear IDE model 5: $Q = 3H\delta\rho_{\rm de}$

When energy flows from dark matter to dark energy ($\delta < 0$), the model may experience $\rho_{\rm dm} < 0$, alongside $w_{\rm dm}^{\rm eff} = \pm\infty$, in the future, as shown in [23] and seen in Figure 1.

Substituting equations (5.60) and (5.61) from [23] into (3) yields:

$$\rho_{\rm D}(z) = \left(\rho_{\rm (dm,0)} + \rho_{\rm (de,0)}\left(\frac{\delta}{\delta + w}\right)\left[1 - (1+z)^{3(\delta+w)}\right]\right)(1+z)^3 + \rho_{\rm (de,0)}(1+z)^{3(\delta+w+1)}. \tag{15}$$

Substituting equations (5.60) and (5.61) from [23] into (4) gives:

$$w_{\rm D}^{\rm eff}(z) = -\,w\,\frac{(\delta + w)\,\Omega_{\rm (de,0)}(1+z)^{3(\delta+w)}}{w\,\Omega_{\rm (de,0)}(1+z)^{3(\delta+w)} + \delta\,\Omega_{\rm (de,0)} + (\delta + w)\,\Omega_{\rm (dm,0)}}. \tag{16}$$

3.6 Non-linear IDE model 1: $Q = 3H\delta\left(\frac{\rho_{\rm dm}\rho_{\rm de}}{\rho_{\rm dm}+\rho_{\rm de}}\right)$

This interaction model always has $\rho_{\rm dm} > 0$ and $\rho_{\rm de} > 0$, with no divergences for either $w_{\rm dm}^{\rm eff}$ or $w_{\rm de}^{\rm eff}$, as shown in [24] and seen in Figure 1.

Substituting equations (4.1) and (4.2) from [24] into (3) yields:

$$\rho_{\rm D}(z) = \left[\rho_{\rm (dm,0)}(1+z)^{3(1-\delta)} + \rho_{\rm (de,0)}(1+z)^{3(1+w)}\right] \left[\frac{1+\left(\frac{\rho_{\rm (dm,0)}}{\rho_{\rm (de,0)}}\right)(1+z)^{-3(w+\delta)}}{1+\left(\frac{\rho_{\rm (dm,0)}}{\rho_{\rm (de,0)}}\right)}\right]^{-\frac{\delta}{w+\delta}}. \tag{17}$$

Substituting equations (4.1) and (4.2) from [24] into (4) gives:

$$w_{\rm D}^{\rm eff}(z) = \frac{w}{1+\left(\frac{\rho_{\rm (dm,0)}}{\rho_{\rm (de,0)}}\right)(1+z)^{-3(w+\delta)}}. \tag{18}$$

3.7 Non-linear IDE model 2: $Q = 3H\delta\left(\frac{\rho_{\rm dm}^2}{\rho_{\rm dm}+\rho_{\rm de}}\right)$

When energy flows from dark matter to dark energy ($\delta < 0$), the model may experience $\rho_{\rm de} < 0$ alongside $w_{\rm de}^{\rm eff} = \pm\infty$ in the past, as shown in [24] and seen in Figure 1.

Substituting equation (4.12) from [24] into (3) yields:

$$\begin{aligned}\rho_{\rm D}(z) = &\left[\rho_{\rm (dm,0)} + \rho_{\rm (de,0)}\left(\frac{\left[w+\delta\left(\frac{\rho_{\rm (dm,0)}}{\rho_{\rm (de,0)}}\right)\right](1+z)^{3w} - \delta\left(\frac{\rho_{\rm (dm,0)}}{\rho_{\rm (de,0)}}\right)}{w}\right)\right](1+z)^{3\left(1-\frac{w\delta}{w-\delta}\right)} \\ &\times\left[\frac{\left[w+\delta\left(\frac{\rho_{\rm (dm,0)}}{\rho_{\rm (de,0)}}\right)\right](1+z)^{3w} + \left(\frac{\rho_{\rm (dm,0)}}{\rho_{\rm (de,0)}}\right)(w-\delta)}{w\left[1+\frac{\rho_{\rm (dm,0)}}{\rho_{\rm (de,0)}}\right]}\right]^{\frac{\delta}{w-\delta}}.\end{aligned} \tag{19}$$

Substituting equation (4.12) from [24] into (4) gives:

$$w_{\rm D}^{\rm eff}(z) = \frac{w}{1+\frac{wr_0}{(w+\delta r_0)a^{-3w}-\delta r_0}}. \tag{20}$$

3.8 Non-linear IDE model 3: $Q = 3H\delta\left(\frac{\rho_{\rm de}^2}{\rho_{\rm dm}+\rho_{\rm de}}\right)$

When energy flows from dark matter to dark energy ($\delta < 0$), the model may experience $\rho_{\rm dm} < 0$, alongside $w_{\rm dm}^{\rm eff} = \pm\infty$, in the future, as shown in [24] and seen in Figure 1.

Substituting equation (4.24) from [24] into (3) yields:

$$\begin{aligned}\rho_{\rm D}(z) = &\left[\rho_{\rm (dm,0)}\left(\frac{\left[w\left(\frac{\rho_{\rm (dm,0)}}{\rho_{\rm (de,0)}}\right)+\delta\right](1+z)^{-3w} - \delta}{w\left(\frac{\rho_{\rm (dm,0)}}{\rho_{\rm (de,0)}}\right)}\right) + \rho_{\rm (de,0)}\right](1+z)^{3\left(1+\frac{w^2}{w-\delta}\right)} \\ &\times\left[\frac{\left[w\left(\frac{\rho_{\rm (dm,0)}}{\rho_{\rm (de,0)}}\right)+\delta\right](1+z)^{-3w} + w - \delta}{w\left(1+\frac{\rho_{\rm (dm,0)}}{\rho_{\rm (de,0)}}\right)}\right]^{\frac{\delta}{w-\delta}}.\end{aligned} \tag{21}$$

Substituting equation (4.24) from [24] into (4) gives:

$$w_{\rm D}^{\rm eff}(z) = \frac{w}{1+\left(r_0+\frac{\delta}{w}\right)a^{3w} - \frac{\delta}{w}}. \tag{22}$$

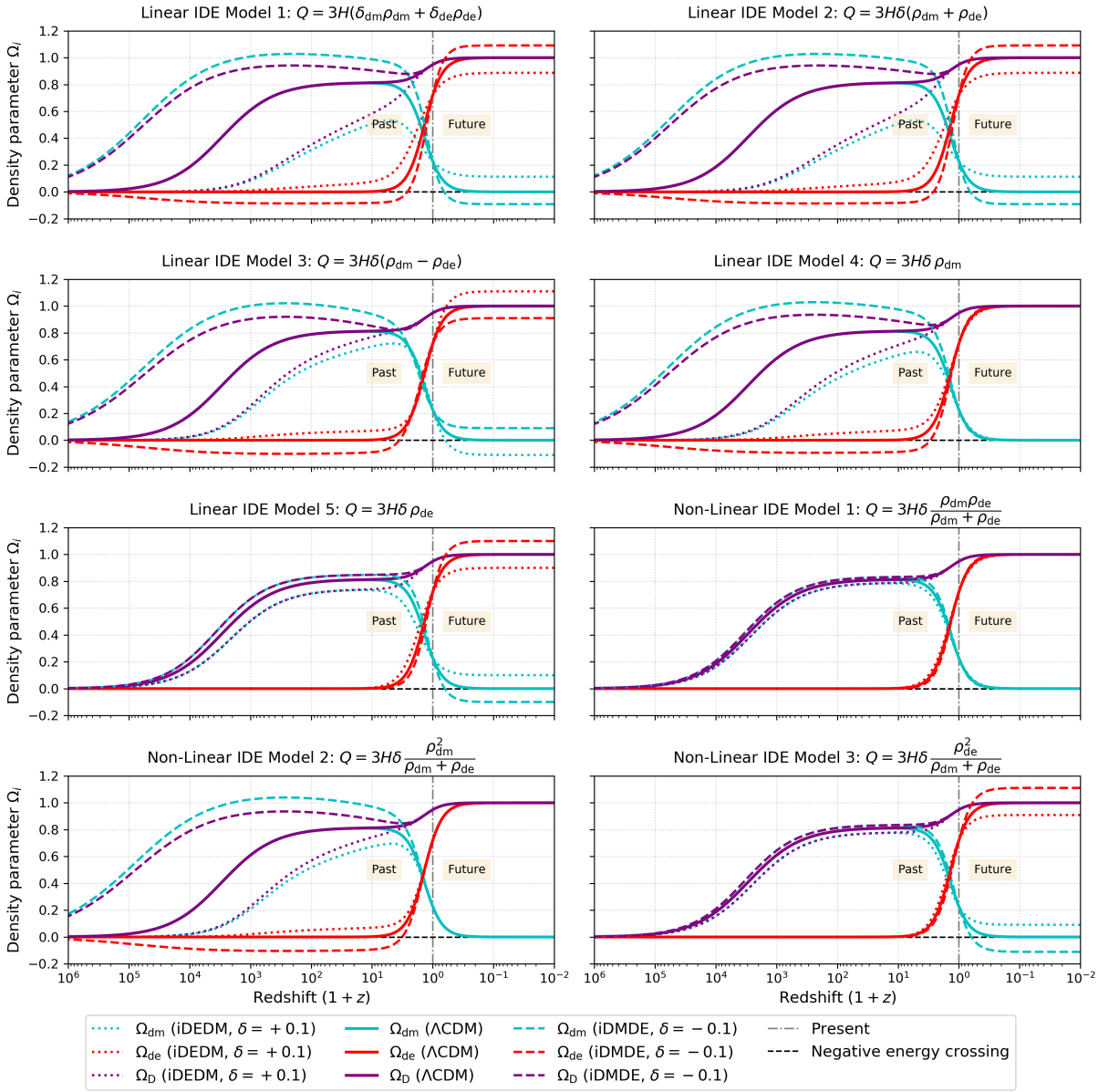


Figure 1: Density parameters for dark matter $\Omega_{\rm dm}$, dark energy $\Omega_{\rm de}$ and unified dark fluid $\Omega_{\rm D}$ vs redshift for each of the 8 IDE models. When energy flows from dark matter to dark energy (iDEDM regime with $\delta < 0$), we see negative dark energy in the past for Linear IDE Model 1, 2, 3, 4 and Non-linear IDE model 2. We also observe negative dark matter densities in the future for Linear IDE Model 1, 2, 3, 5 and Non-linear IDE model 3. In all eight cases, we can see that although the individual components may become negative, the total fluid as given by the unified dark fluid description in section 3 remains positive at all times.

.

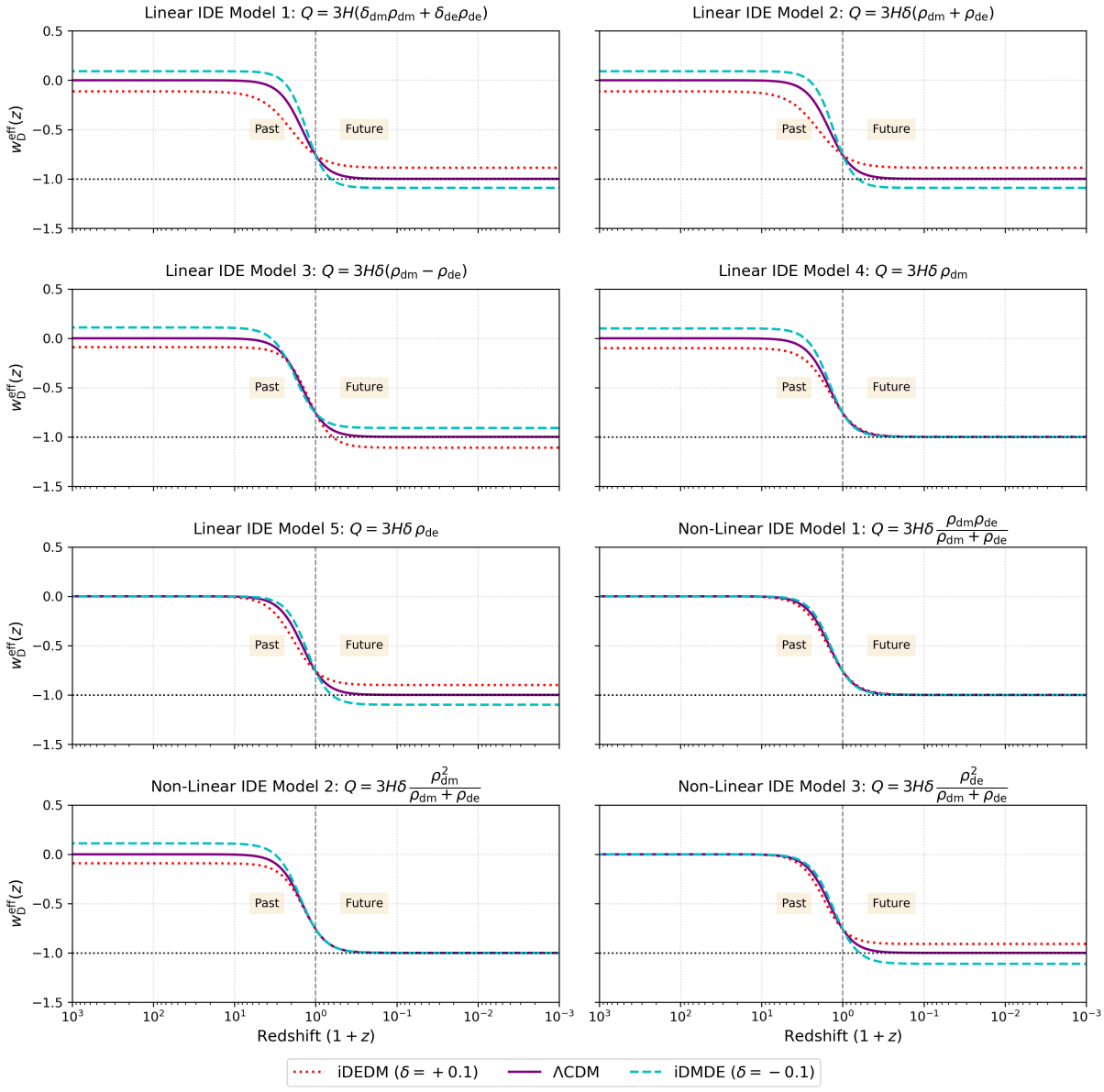


Figure 2: Dark fluid equation of state $w_{\rm D}^{\rm eff}(z)$ vs redshift for each of the 8 IDE models, given a unified dark fluid description $w_{\rm D}^{\rm eff}(z) = \frac{p_{\rm D}}{\rho_{\rm D}} = \frac{w\rho_{\rm de}(z)}{\rho_{\rm dm}(z)+\rho_{\rm de}(z)}$, showing no divergent behaviour in either regime ($\delta = \pm 0.1$). This is in contrast to the divergences expected for the effective equations of state for dark matter $w_{\rm dm}^{\rm eff}$ and dark energy $w_{\rm de}^{\rm eff}$ when the dark matter or dark energy crosses into negative values respectively, as illustrated in [23, 24].

3.9 A short analysis of the evolution of $\rho_D(z)$ and $w_{\rm D}^{\rm eff}(z)$

The evolution of the energy densities in section 3 can be expressed in terms of density parameters ($\frac{8\pi G}{3H^2}\rho_i = \Omega_i$) and are plotted in Figure 1. For all figures, the input parameters are $H_0 = 67.4$ km/s/Mpc, $\Omega_{(\rm r,0)} = 9 \times 10^{-5}$, $\Omega_{(\rm bm,0)} = 0.049$, $\Omega_{(\rm dm,0)} = 0.266$, $\Omega_{(\rm de,0)} = 0.685$, $w = -1$, and $\delta = \pm 0.1$, unless stated otherwise. As previously noted, we see $\Omega_{\rm de} < 0$ in the past for Linear IDE Model 1, 2, 3, 4 and Non-linear IDE model 2, while $\Omega_{\rm dm} < 0$ in the future for Linear IDE Model 1, 2, 3, 5 and Non-linear IDE model 3. In all cases the UDF density parameter $\Omega_{\rm D} > 0$ for all z, while asymptotically approaching $\Omega_{\rm D} \to 0$ in the past, and $\Omega_{\rm D} \to 1$ in the future.

In Figure 2, we see this is accompanied by the UDF equation of state $w_{\rm D}^{\rm eff}(z)$ avoiding singularities characteristic of $w_{\rm dm}^{\rm eff}(z)$ and $w_{\rm de}^{\rm eff}(z)$ in IDE cosmologies when $\delta < 0$. In the past, $w_{\rm de}^{\rm eff}(z)$ nearly mimics cold dark matter behaviour, while approaching a dark energy type phase in the future, similar to Chaplygin Gas models. The exact asymptotic past and future values of $w_{\rm de}^{\rm eff}(z)$ for all models is summarized in Table 2.

Table 2 shows that different interaction kernels lead to unified dark fluid equations of state with distinct asymptotic behaviours. In particular, some models exhibit both non-cold dark matter behaviour in the asymptotic past ($w_{\rm D,past}^{\rm eff} \neq 0$) followed by non-cosmological constant ($w_{\rm D,past}^{\rm eff} \neq w = -1$) accelerating phase in the future, while others display the opposite behaviour or agree in one of the cases. These possibilities may be characteristic of a wide class of other models, including dynamical dark energy models [58], modification to gravity [59] and generalized and modified Chaplygin gas cosmologies [29, 51, 55, 60, 61], the last of which we will consider in the next section. In this sense, interacting dark energy models can be viewed as a specific decomposition for several phenomenological unified dark fluid behaviours at the background level.

Table 2: Asymptotic past, present, and future values of $w_{\rm D}^{\rm eff}(z)$ for various interaction models Q. The determinant Δ in the first three rows is found in sections 3.1, 3.2 and 3.3, respectively. We find that for all cases the UDF equation of state in the past is equal to the effective dark matter equation of state $w_{\rm D,past}^{\rm eff} = w_{\rm dm,past}^{\rm eff}$, while in the future being equal to the effective dark energy equation of state $w_{\rm D,future}^{\rm eff} = w_{\rm de,future}^{\rm eff}$. The evolution of $w_{\rm dm}^{\rm eff}(z)$ and $w_{\rm de}^{\rm eff}(z)$ as well as their asymptotic values can be found in [23, 24]

Interaction Q	$w_{\rm D,past}^{\rm eff}$	$w_{\rm D,present}^{\rm eff}$	$w_{\rm D,future}^{\rm eff}$
$3H(\delta_{\rm dm}\rho_{\rm dm} + \delta_{\rm de}\rho_{\rm de})$	$\frac{1}{2}(\delta_{\rm de} - \delta_{\rm dm} + w + \Delta)$	$\frac{w}{1+r_0}$	$\frac{1}{2}(\delta_{\rm de} - \delta_{\rm dm} + w - \Delta)$
$3H\delta(\rho_{\rm dm} + \rho_{\rm de})$	$\frac{1}{2}(w + \Delta)$	$\frac{w}{1+r_0}$	$\frac{1}{2}(w - \Delta)$
$3H\delta(\rho_{\rm dm} - \rho_{\rm de})$	$\frac{1}{2}(2\delta + w + \Delta)$	$\frac{w}{1+r_0}$	$\frac{1}{2}(2\delta + w - \Delta)$
$3H\delta\rho_{\rm dm}$	$-\delta$	$\frac{w}{1+r_0}$	w
$3H\delta\rho_{\rm de}$	0	$\frac{w}{1+r_0}$	$w + \delta$
$3H\delta\left(\frac{\rho_{\rm dm}\rho_{\rm de}}{\rho_{\rm dm}+\rho_{\rm de}}\right)$	0	$\frac{w}{1+r_0}$	w
$3H\delta\left(\frac{\rho_{\rm dm}^2}{\rho_{\rm dm}+\rho_{\rm de}}\right)$	$\frac{\delta w}{\delta - w}$	$\frac{w}{1+r_0}$	w
$3H\delta\left(\frac{\rho_{\rm de}^2}{\rho_{\rm dm}+\rho_{\rm de}}\right)$	0	$\frac{w}{1+r_0}$	$\frac{w^2}{w-\delta}$

4 Connection to Chaplygin Gas Models

4.1 Relating $Q = 3H\delta\left(\frac{\rho_{\rm dm}\rho_{\rm de}}{\rho_{\rm dm}+\rho_{\rm de}}\right)$ to the Generalized Chaplygin Gas (GCG) model

Chaplygin gas models try to unify both dark matter and dark energy into a single exotic fluid, which has a dynamic equation of state [51, 55, 60–62], acting like matter at early times and a cosmological constant at late times . A connection between IDE models and Chaplygin gas cosmology has been noted before [51, 55, 60–62].

For our purpose, a previous connection between a specific IDE kernel $Q = 3\delta H\left(\frac{\rho_{\rm dm}\rho_{\rm de}}{\rho_{\rm dm}+\rho_{\rm de}}\right)$ and CG model was noted in Figure 19 of [24], where it was mentioned that the IDE model showcases similar trajectories of the statefinder parameters in the q vs. r and s vs. r planes, as the Chaplygin gas model shown in Figure 1 of [63]. From this motivation, we construct a simple transformation below between this interaction kernel and CG model.

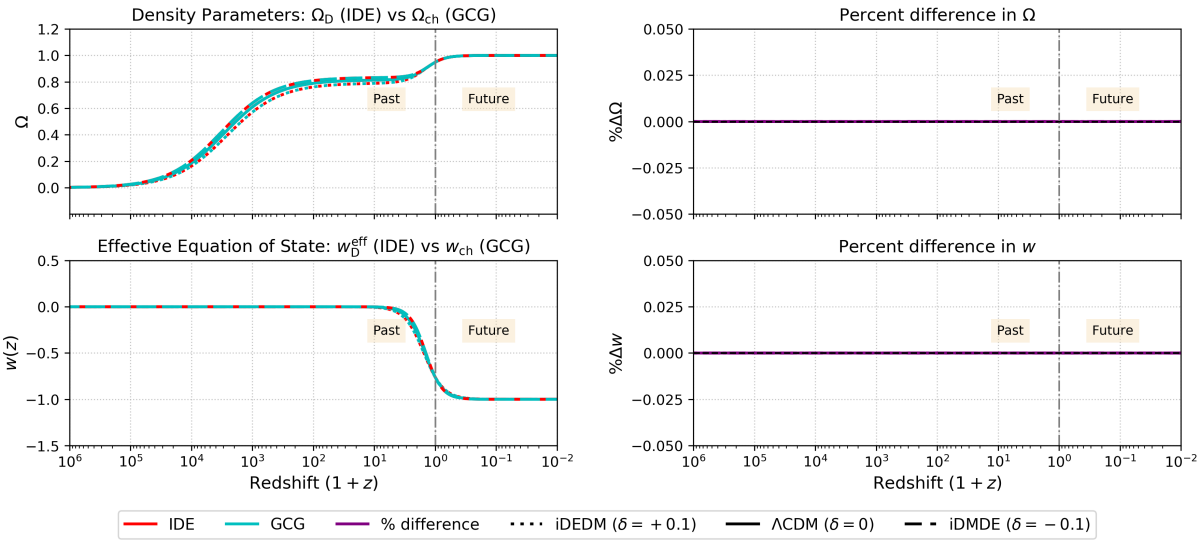


Figure 3: Equivalence of UDF description of IDE model $Q = 3H\delta\left(\frac{\rho_{\rm dm}\rho_{\rm de}}{\rho_{\rm dm}+\rho_{\rm de}}\right)$ described by (17) and (18) and the Generalized Chaplygin Gas (GCG) model described by (24) and (25) under transformation (29). Density parameters (top left panel), percentage difference between density parameters (top right panel), equation of state (bottom left panel) and percentage difference between equations of state (bottom right panel) vs redshift. In all four panels, we see the same evolution and may conclude that the IDE model and GCG are equivalent under transformation (29).

One of the simplest models is the Generalized Chaplygin Gas (GCG) model [51, 64–67], which has a pressure p:

$$p = -\frac{A}{\rho_{\rm ch}^{\alpha}}, \tag{23}$$

where A is a constant that needs to be positive to ensure accelerated expansion, α is a second constant that describes the type of model, and $\rho_{\rm ch}$ is the energy density, equivalent to [67]:

$$\rho_{\rm ch}(z) = \rho_{(\rm ch,0)}\left[A_s + (1-A_s)(1+z)^{3(1+\alpha)}\right]^{\frac{1}{1+\alpha}}, \tag{24}$$

with $A_s = A/\rho_{(\rm ch,0)}^{1+\alpha}$. For the special cases where $A_s = 1$ or $A_s = 0$ (for any value of α), the GCG behaves like either a standard cosmological constant with $w = -1$, or pressureless dark matter with $w = 0$ throughout all of cosmological evolution [67]. When $\alpha = 0$, we obtain a UDF description of ΛCDM, and when $\alpha = 1$, we obtain the original Chaplygin gas model [51, 64]. The equation of state for the GCG fluid is given by [67]:

$$w_{\rm ch}(z) = -\frac{A_s}{A_s + (1-A_s)(1+z)^{3(1+\alpha)}}, \tag{25}$$

which at present gives $w(0) = -A_s$. Equivalence with the UDF equation of state ($w_{\rm D,present}^{\rm eff}$ in Table 2) requires:

$$A_s = -\frac{w}{1+r_0} \tag{26}$$

Substituting (26) into (25), and simplifying gives:

$$w_{\rm ch}(z) = \frac{w}{1+r_0(1+z)^{3(1+\alpha)}}, \tag{27}$$

Comparing (27) with (18), we find that $w_{\rm ch} = w_{\rm D}^{\rm eff}$ given that:

$$1+\alpha = -(w+\delta) \quad \rightarrow \quad \alpha = -(w+\delta+1). \tag{28}$$

Since both models have the same conservation equation, we should find that $\rho_{\rm D} = \rho_{\rm ch}$ for all z, provided both share the same initial conditions. We demonstrate that the IDE interaction $Q = 3H\delta\,\frac{\rho_{\rm dm}\rho_{\rm de}}{\rho_{\rm dm}+\rho_{\rm de}}$ is exactly equivalent,

at the background level, to a generalized Chaplygin gas model under the transformation (29):

$$\boxed{\text{IDE model } Q = 3H\delta\,\frac{\rho_{\rm dm}\rho_{\rm de}}{\rho_{\rm dm}+\rho_{\rm de}} = \text{ Generalized Chaplygin Gas (GCG) model at the background level, if:}}$$
$$\rho_{\rm D,0} = \rho_{\rm dm,0} + \rho_{\rm de,0}, \qquad A_s = -\frac{w}{1+r_0}, \qquad \alpha = -(w+\delta+1) \tag{29}$$

From (29), we can immediately see that in the case where $w = -1$ and $\delta = 0$, we obtain $\alpha = 0$, corresponding to the ΛCDM case [51, 64]. The equivalence over a wide redshift of both the energy densities and effective equation of state of the IDE model described by (17) and (18), and the GCG model described by (24) and (25) under transformation (29), is illustrated in Figure 3.

5 Brief implications from observational constraints

In a recent study [33], late-time probes were used to find background observational constraints on the eight IDE models studied in this paper. This study also showed that for all models possible, there is a phantom-divide crossing in the effective dark energy equation of state $w_{\rm de}^{\rm eff}$, showcasing quintessence behaviour $w_{\rm de}^{\rm eff} > -1$ at low redshift and phantom behaviour at $w_{\rm de}^{\rm eff} < -1$ at higher redshift.

Using the posteriors from Table IV and V in [33] as input for our cosmological parameters, we may see how $w_{\rm D}^{\rm eff}(z)$ evolves in Figure 4, which can be compared to Figure 7 in [33]. For all eight models, no phantom crossing is expected for the UDF description, but instead quintessence-like behaviour $w_{\rm D}^{\rm eff} > -1$ is observed at present and low redshift. At higher redshift, we see that cold dark matter behaviour is recovered, with $w_{\rm D}^{\rm eff} \approx 0$.

Lastly, in Table 3 we use the transformation (29) to infer the mean values for the GCG model at the background level from the observational posteriors for IDE model $Q = 3H\delta\,\frac{\rho_{\rm dm}\rho_{\rm de}}{\rho_{\rm dm}+\rho_{\rm de}}$, found in Table IV and V in [33]. As this is simply illustrative, we will ignore the error margins associated with the parameter values. From Table 3, we see that $0 < A_s < 1$ and $\alpha > -1$, which corresponds to the standard GCG model, behaving like dust ($w = 0$) at high redshift, while approaching cosmological constant behaviour ($w = -1$) asymptotically into the future, which is in agreement with Table 2. Different cosmological scenarios corresponding to different combinations of A_S and α can be found in [67]. We emphasize that the results in Table 3 are mapped values evaluated at the posterior level, rather than independent statistical constraints on the GCG model.

Table 3: For illustrative purposes, a mapping is presented between the non-linear IDE model $Q = 3H\delta\,\rho_{\rm dm}\rho_{\rm de}/(\rho_{\rm dm}+\rho_{\rm de})$ and the equivalent Generalized Chaplygin Gas (GCG) model at the background level. The mean values are inferred from the observational posteriors in Table IV and V in [33] using the transformation (29).

Dataset	$\boldsymbol{\Omega_{\rm dm,0}}$	$\boldsymbol{\Omega_{\rm b,0}}$	$\boldsymbol{w}$	$\boldsymbol{\delta}$	$\boldsymbol{\Omega_{\rm D,0}}$	$\boldsymbol{A_s}$	$\boldsymbol{\alpha}$
Pantheon+ & DESI DR2	0.074	0.048	−0.711	−0.85	0.9519	0.6557	0.561
Pantheon+, DESI DR2, CC & BBN	0.083	0.0449	−0.731	−0.78	0.9550	0.6675	0.511

6 Discussions and Conclusions

In this work, we have shown in section 2 and 3 that a reformulation of dark sector interaction as a unified dark fluid with a dynamical equation of state, can provide an interpretation of IDE models where negative dark matter and dark energy densities are less problematic at the background level. This is illustrated in both Figure 1 and Figure 2, which shows that at all times the total dark sector remains positive and divergent equation of state behaviour is avoided. This UDF interpretation opens up the parameter space, including sections which are associated with energy transfer from dark matter to dark energy, and thus increase the potential of models to address tensions in cosmology. We emphasize that this does not remove negative densities in the standard two–fluid description of IDE models. Rather, it shows that these features need not represent fundamental pathologies of the background cosmology, but instead arise from the particular decomposition of the dark sector into interacting components. The unified dark fluid description therefore provides an alternative, physically consistent interpretation of the same background dynamics.

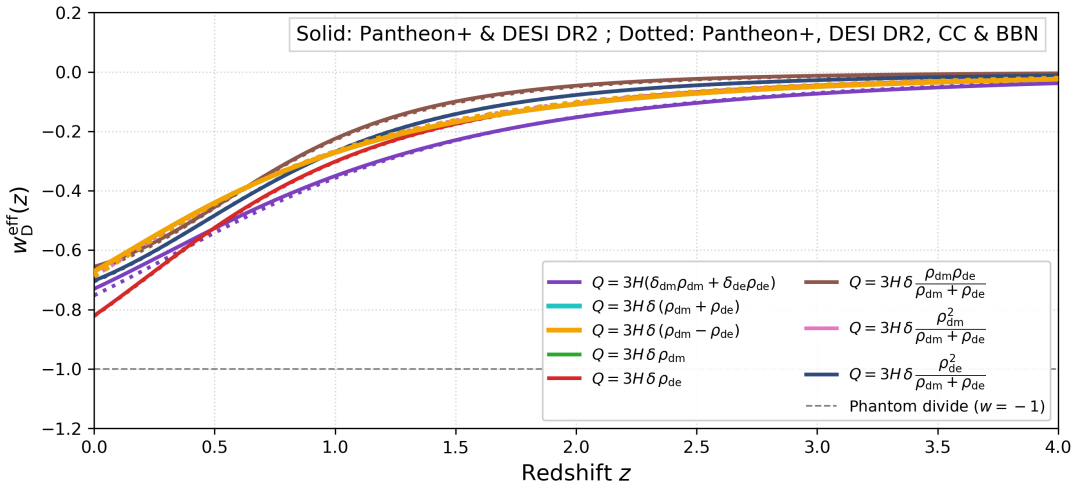


Figure 4: Evolution of the effective unified dark fluid equations of state $w_{\rm D}^{\rm eff}(z)$ for all eight interaction models, using the mean values reported in Tables IV and V of [33]. We observe no phantom-divide crossing, but instead observe quintessence behaviour $w_{\rm D}^{\rm eff} > -1$ at present and low redshift, while CDM behaviour $w_{\rm D}^{\rm eff} \approx 0$ is observed at higher redshift, for all models.

In section 4, we derived the new correspondence given in (29) and illustrated in Figure 3. This transformation was used in section 5 to perform a mapping at the posterior level of previous observational constraints obtained for an IDE model to a GCG model to produce Table 3, which serves as an example of how constraints on one model may be used to understand another model. The correspondence suggests that several interacting dark energy scenarios can be interpreted as specific realizations within a broader unified dark fluid framework, of which the Generalized Chaplygin Gas represents a particular limiting case. Another example that has been noted in [55], is an equivalence between the same interaction $Q = 3H\delta\left(\frac{\rho_{\rm dm}\rho_{\rm de}}{\rho_{\rm dm}+\rho_{\rm de}}\right)$ and the new generalized Chaplygin gas (NGCG) scenario. Future work may consider similar mappings between IDE models and other Chaplygin gas models, such as the previously mentioned NGCG, as well as modified Chaplygin gas (MCG) models [68, 69]. The asymptotic past and future behavior of the effective equation of state of the single fluid, shown in Table 2, particularly in cases where $w_{\rm D}^{\rm eff}(z) \neq w$, may help identify additional mappings that have not yet been explored.

Given these considerations, IDE, UDF, and CG models may be viewed as alternative parametrizations of the same background expansion history, with differences becoming physically meaningful only once perturbations are considered. Thus, at the background level, we may use observational constraints on IDE models to understand UDF behaviour, and, for example, if it permits phantom crossings as seen in Figure 4. Alternatively, we may view an IDE model as a particular decomposition of a unified fluid into interacting subcomponents, as done in [54]. Here it is also discussed how to break degeneracies of UDF models with CPL descriptions of dark energy using non-linear regimes. This is done for example, by analysing not only linear perturbations, but predictions for spherical collapse (see [70] for a recent example of this for IDE models) and Halo mass functions. Similar considerations to break degeneracies for IDE models are found in [53] and may also be done in a future work. This would enable us to determine both the relevance of IDE models for addressing urgent questions in cosmology, as well as the ability to distinguish its effects among a myriad of similar models.

Appendix A: A brief note on perturbations in UDF and IDE models

The analysis presented in the main text is restricted to the homogeneous background evolution. This is sufficient for demonstrating the background-level equivalence between the interacting dark energy models considered here and a unified dark fluid description. However, background equivalence does not guarantee perturbative equivalence. This is closely related to the dark degeneracy, namely that different dark-sector descriptions can generate the same background expansion history while differing once perturbations are specified [50, 52, 53]. At the level of cosmological perturbations, the dynamical behaviour of a single unified fluid depends on additional information, such as its rest-frame sound speed $c_{s,D}^2$, non-adiabatic pressure perturbation, and anisotropic stress [54, 71]. Similarly, in the two-fluid interacting description, perturbations depend not only on the background interaction kernel Q, but also on the covariant interaction four-vector Q_A^μ, including its perturbation δQ and the choice of momentum-

transfer frame (e.g. parallel to the dark matter or dark energy four-velocity) [18, 19, 55]. The background mapping fixes only the homogeneous density and pressure of the dark sector, leaving its perturbative degrees of freedom undetermined. Although the total density and pressure perturbations are obtained by summing those of the individual dark components, this does not determine the effective pressure perturbation of the unified fluid, which additionally depends on its rest-frame sound speed and entropy perturbations [54, 71]. Likewise, the total velocity perturbation depends on the relative velocities of the dark matter and dark energy components, information that has no unique counterpart in the unified-fluid description. Consequently, two models with the same background expansion history $H(z)$ may nevertheless predict different growth histories, matter power spectra, and metric perturbations once their perturbation prescriptions are specified [52–55]. Perturbative equivalence is therefore not ruled out, but it requires additional, non-unique assumptions beyond the background mapping.

Another issue is that of the treatment of sound speed in the single and two fluid cases. For a unified dark fluid with equation of state $w_{\rm D} = p_{\rm D}/\rho_{\rm D}$, the adiabatic sound speed is defined by $c^2_{a,D} \equiv \dot{p}_{\rm D}/\dot{\rho}_{\rm D}$. Using $p_{\rm D} = w_{\rm D}\rho_{\rm D}$ together with the conservation equation (2), one obtains

$$c^2_{a,D} = w_{\rm D} - \frac{\dot{w}_{\rm D}}{3H(1+w_{\rm D})}, \tag{30}$$

whenever $w_{\rm D} \neq -1$. For a barotropic fluid, the adiabatic and rest-frame sound speeds coincide, $c^2_{s,D} = c^2_{a,D}$. However, dark energy is generally treated as a non-adiabatic fluid in perturbation theory, so that its rest-frame sound speed $c^2_{s,\rm de}$ is specified independently of $c^2_{a,\rm de}$. In phenomenological interacting dark energy models it is customary to choose $c^2_{s,\rm de} = 1$, in order to avoid the instabilities that would arise if $c^2_{s,\rm de} = c^2_{a,\rm de} = w_{\rm de} < 0$ [55]. By contrast, unified dark fluid models may assume a vanishing rest-frame sound speed, $c^2_{s,D} \simeq 0$, together with negligible anisotropic stress, so that the fluid clusters like cold dark matter at early times while remaining compatible with current cosmological observations, even though this choice does not in general reproduce the perturbations of a given interacting or dynamical dark energy model [54].

A similar result can be found for the decomposed new generalized Chaplygin gas (NGCG) model and interacting fluid models. It is shown in [55] that the interaction model discussed in Section 4,

$$Q = 3H\delta\left(\frac{\rho_{\rm dm}\rho_{\rm de}}{\rho_{\rm dm}+\rho_{\rm de}}\right), \tag{31}$$

is equivalent to a decomposed NGCG model. In the notation of [55], the interaction is written with coupling β, while in our convention the corresponding coupling is $\delta = -\beta$. The same work also relates the NGCG parameter α to the interacting description through $\beta = -\alpha w$. In that convention, stable cosmological perturbations were found for $\beta > 0$ with $w > -1$, which corresponds in our notation to $\delta < 0$ with $w > -1$.

This stability condition can also be understood from the doom-factor **d** diagnostic introduced in [19], for which $\mathbf{d} > 0$ may signal the presence of early-time non-adiabatic instabilities in the dark energy perturbations within the standard fluid description. For the sign convention used in this paper, the doom factor is

$$\mathbf{d} = \frac{Q}{3H\rho_{\rm de}(1+w)} = \frac{\delta}{1+w}\frac{\rho_{\rm dm}}{\rho_{\rm dm}+\rho_{\rm de}}, \tag{32}$$

where we have substituted the non-linear interaction Q from (31). As shown in the main text, all energies are always positive for this interaction, thus implying that the factor $\rho_{\rm dm}/(\rho_{\rm dm}+\rho_{\rm de})$ is positive. Hence the sign of d is controlled by $\delta/(1+w)$. The doom-factor stability criteria $d < 0$ therefore requires

$$\delta(1+w) < 0. \tag{33}$$

Equivalently, there are two combinations of parameters that are a priori stable:

$$\delta > 0 \text{ (iDEDM regime) with } w < -1, \qquad \text{or} \qquad \delta < 0 \text{ (iDMDE regime) with } w > -1. \tag{34}$$

The second combination is the stable $\beta > 0$, $w > -1$ result found in [55], given the notation difference. The first combination was not considered in that paper, but is also stable in accordance with the doom-factor criterion, and corresponds to energy transfer from dark energy to dark matter with a phantom dark energy equation of state. Thus, for the non-linear interaction (31), the doom factor analysis gives the compact stability condition (33), provided the evolution remains on the branch where the total dark sector is positive, which is discussed in Appendix B: Domain of validity of the UDF description.

A full perturbative analysis is beyond the scope of the present proceedings, and the equivalence demonstrated here should be understood as a background-level equivalence. Perturbations for interacting dark energy models are still an active area of research, with extensions beyond the fluid framework found in [62, 72, 73], while new developments on linear and non-linear growth are found in [31, 74–78].

Appendix B: Domain of validity of the UDF description

The positivity argument following (5) applies to the regular UDF branch, where the total dark sector density $\rho_{\rm D}(a)$ defined in (3) remains positive and the effective equation of state $w_{\rm D}^{\rm eff}(z)$ in (4) remains finite. This is the regime considered in the main text, where negative values of the individual dark matter or dark energy densities in the two-fluid decomposition do not necessarily imply a negative total dark fluid. The UDF formulation thus avoids the negative energies associated with energy transfer from dark matter to dark energy (iDMDE regime), as detailed in [23, 24].

This should be distinguished from the more problematic Strong interacting Dark Energy Dark Matter (SiDEDM) regime discussed in [79], where the conditions for the IDE models studied in this paper to enter this problematic regime are also given. In that regime, the interaction is sufficiently large, such that $\rho_{\rm dm}$ or $\rho_{\rm de}$ may become negative enough that the total dark sector density $\rho_{\rm D}$ also crosses zero. At such a crossing, the denominator of (4) vanishes and $w_{\rm D}^{\rm eff}$ is not well defined. The SiDEDM solutions do not contradict the positivity result obtained from (5). Instead, these solutions fall outside the assumptions under which the single-fluid UDF description is defined at all times. In this sense, the positive energy arguments arising from (5) should be understood as applying only to weak dark sector interactions where both $\rho_{\rm D} > 0$ and $|w_{\rm D}^{\rm eff}| < \infty$ throughout past and future expansion. The conditions for the IDE models studied in this paper to enter this problematic regime are discussed in [79].

This also clarifies the relation to cosmological turnarounds. In a flat FLRW universe, a turnaround occurs when the total cosmic density reaches zero $\rho_{\rm tot} = 0$, so that $H = 0$. Since baryons and radiation contribute positively, the dark sector must become sufficiently negative $\rho_{\rm D} < 0$, to cancel these positive components. Thus, turnarounds associated with crunching and bouncing cosmologies with an effective negative dark sector contribution can occur in the SiDEDM regime [79], but these solutions are not part of the positive, regular UDF branch associated with the weakly interacting iDMDE and iDEDM regimes studied in the present work.

Acknowledgements

MvdW would like to thank the Centre for Space Research at North-West University (NWU) for funding during the academic year 2025, which enabled the research that is presented in this study and the attendance of the SAGS2025 conference.

References

[1] M. Abdul Karim et al. DESI DR2 results. II. Measurements of baryon acoustic oscillations and cosmological constraints. *Phys. Rev. D*, 112(8):083515, 2025.

[2] M. Abdul Karim et al. DESI DR2 results. I. Baryon acoustic oscillations from the Lyman alpha forest. *Phys. Rev. D*, 112(8):083514, 2025.

[3] Eleonora Di Valentino, Alessandro Melchiorri, Olga Mena, and Sunny Vagnozzi. Interacting dark energy in the early 2020s: A promising solution to the H_0 and cosmic shear tensions. *Phys. Dark Univ.*, 30:100666, 2020.

[4] Eleonora Di Valentino et al. The CosmoVerse White Paper: Addressing observational tensions in cosmology with systematics and fundamental physics, 4 2025.

[5] Dily Duan Yi Ong and Will Handley. `unimpeded`: A Public Grid of Nested Sampling Chains for Cosmological Model Comparison and Tension Analysis, 11 2025.

[6] Luca Amendola. Coupled quintessence. *Phys. Rev. D*, 62:043511, 2000.

[7] Winfried Zimdahl and Diego Pavon. Interacting quintessence. *Phys. Lett. B*, 521:133–138, 2001.

[8] Luis P. Chimento, Alejandro S. Jakubi, Diego Pavon, and Winfried Zimdahl. Interacting quintessence solution to the coincidence problem. *Phys. Rev. D*, 67:083513, 2003.

[9] Eleonora Di Valentino, Olga Mena, Supriya Pan, Luca Visinelli, Weiqiang Yang, Alessandro Melchiorri, David F. Mota, Adam G. Riess, and Joseph Silk. In the realm of the Hubble tension—a review of solutions. *Class. Quant. Grav.*, 38(15):153001, 2021.

[10] Eleonora Di Valentino and Olga Mena. A fake Interacting Dark Energy detection? *Mon. Not. Roy. Astron. Soc.*, 500(1):L22–L26, 2020.

[11] Eleonora Di Valentino, Alessandro Melchiorri, Olga Mena, and Sunny Vagnozzi. Interacting dark energy in the early 2020s: A promising solution to the H_0 and cosmic shear tensions. *Phys. Dark Univ.*, 30:100666, 2020.

[12] Sêcloka L. Guedezounme, Bikash R. Dinda, and Roy Maartens. Phantom crossing or dark interaction?, 7 2025.

[13] Supriya Pan, Sivasish Paul, Emmanuel N. Saridakis, and Weiqiang Yang. Interacting dark energy after DESI DR2: a challenge for ΛCDM paradigm?, 4 2025.

[14] Marcel van der Westhuizen, David Figueruelo, Rethabile Thubisi, Shambel Sahlu, Amare Abebe, and Andronikos Paliathanasis. Compartmentalization in the dark sector of the universe after DESI DR2 BAO data. *Phys. Dark Univ.*, 50:102107, 2025.

[15] Marcel A. van der Westhuizen and Amare Abebe. Interacting dark energy: clarifying the cosmological implications and viability conditions. *JCAP*, 01:048, 2024.

[16] Elsa M. Teixeira, Gaspard Poulot, Carsten van de Bruck, Eleonora Di Valentino, and Vivian Poulin. Alleviating cosmological tensions with a hybrid dark sector. *Phys. Rev. D*, 113(2):023514, 2026.

[17] Tian-Nuo Li, William Giarè, Guo-Hong Du, Yun-He Li, Eleonora Di Valentino, Jing-Fei Zhang, and Xin Zhang. Strong Evidence for Dark Sector Interactions, 1 2026.

[18] Jussi Valiviita, Elisabetta Majerotto, and Roy Maartens. Instability in interacting dark energy and dark matter fluids. *JCAP*, 07:020, 2008.

[19] M.B. Gavela, D. Hernández, L. Lopez Honorez, O. Mena, and S. Rigolin. Dark coupling. *Journal of Cosmology and Astroparticle Physics*, 2009(07):034, jul 2009.

[20] Laura Lopez Honorez, Beth A Reid, Olga Mena, Licia Verde, and Raul Jimenez. Coupled dark matter-dark energy in light of near universe observations. *Journal of Cosmology and Astroparticle Physics*, 2010(09):029–029, September 2010.

[21] Gabriela Caldera-Cabral, Roy Maartens, and L. Arturo Urena-Lopez. Dynamics of interacting dark energy. *Phys. Rev. D*, 79:063518, 2009.

[22] Gabriela Caldera-Cabral, Roy Maartens, and Bjoern Malte Schaefer. The growth of structure in interacting dark energy models. *Journal of Cosmology and Astroparticle Physics*, 2009(07):027–027, July 2009.

[23] Marcel van der Westhuizen, Amare Abebe, and Eleonora Di Valentino. I. Linear interacting dark energy: Analytical solutions and theoretical pathologies. *Phys. Dark Univ.*, 50:102119, 2025.

[24] Marcel van der Westhuizen, Amare Abebe, and Eleonora Di Valentino. II. Non-Linear Interacting Dark Energy: Analytical Solutions and Theoretical Pathologies. *Phys. Dark Univ.*, 50:102120, 2025.

[25] Marcel van der Westhuizen, Amare Abebe, and Eleonora Di Valentino. III. Interacting Dark Energy: Summary of models, Pathologies, and Constraints. *Phys. Dark Univ.*, 50:102121, 2025.

[26] E. Aydiner. Chaotic Interaction Between Dark Matter and Dark Energy. *Int. J. Theor. Phys.*, 64(1):3, 2025.

[27] A. A. Escobal, F. B. Abdalla, J. F. Jesus, E. Abdalla, C. Feng, and J. A. S. Lima. A microphysically inspired approach to dark matter-dark energy interactions: first bounds on dark-sector scattering cross sections, 1 2026.

[28] Amin Aboubrahim and Pran Nath. Upper limits on dark energy-dark matter interaction from DESI DR2 in a field-theoretic analysis. *JCAP*, 10:081, 2025.

[29] Yun-He Li, Jing-Fei Zhang, and Xin Zhang. Parametrized Post-Friedmann Framework for Interacting Dark Energy. *Phys. Rev. D*, 90(6):063005, 2014.

[30] Yun-He Li and Xin Zhang. IDECAMB: an implementation of interacting dark energy cosmology in CAMB. *JCAP*, 09:046, 2023.

[31] Emanuelly Silva, Gabriel Hartmann, and Rafael C. Nunes. One-loop power spectrum corrections in interacting dark energy cosmologies. *Phys. Rev. D*, 113(6):063548, 2026.

[32] Matteo Lucca. Dark energy–dark matter interactions as a solution to the S8 tension. *Phys. Dark Univ.*, 34:100899, 2021.

[33] David Figueruelo, Marcel van der Westhuizen, Amare Abebe, and Eleonora Di Valentino. Late-time background constraints on linear and non-linear interacting dark energy after DESI DR2. *Phys. Dark Univ.*, 52:102238, 2026.

[34] Luca Visinelli, Sunny Vagnozzi, and Ulf Danielsson. Revisiting a negative cosmological constant from low-redshift data. *Symmetry*, 11(8):1035, 2019.

[35] Özgür Akarsu, Suresh Kumar, Emre Özülker, and J. Alberto Vazquez. Relaxing cosmological tensions with a sign switching cosmological constant. *Phys. Rev. D*, 104(12):123512, 2021.

[36] Davide Pedrotti, Luis A. Escamilla, Valerio Marra, Leandros Perivolaropoulos, and Sunny Vagnozzi. BAO miscalibration cannot rescue late-time solutions to the Hubble tension. *Phys. Rev. D*, 113(4):043507, 2026.

[37] Mariam Bouhmadi-López and Beñat Ibarra-Uriondo. Cosmological perturbations for smooth sign-switching dark energy models, 6 2025.

[38] Adrià Gómez-Valent and Alex González-Fuentes. Effective phantom divide crossing with standard and negative quintessence. *Phys. Lett. B*, 872:140096, 2026.

[39] Alex González-Fuentes and Adrià Gómez-Valent. Reconstruction of dark energy and late-time cosmic expansion using the Weighted Function Regression method, 6 2025.

[40] Payam Ghafari, Mahdi Najafi, Mina Ghodsi Yengejeh, Emre Özülker, Eleonora Di Valentino, and Javad T. Firouzjaee. A Multi-Probe ISW Study of Dark Energy Models with Negative Energy Density: Galaxy Correlations, Lensing Bispectrum, and Planck ISW-Lensing Likelihood, 12 2025.

[41] Hao Wang and Yun-Song Piao. Impact of a negative cosmological constant on the reconstruction of dark energy in light of DESI BAO data, 1 2026.

[42] J. S. Farnes. A unifying theory of dark energy and dark matter: Negative masses and matter creation within a modified ΛCDM framework. *Astron. Astrophys.*, 620:A92, 2018.

[43] Hector Socas-Navarro. Can a negative-mass cosmology explain dark matter and dark energy? *Astron. Astrophys.*, 626:A5, 2019.

[44] Sebastián Nájera, Aldo Gamboa, Alejandro Aguilar-Nieto, and Celia Escamilla-Rivera. On negative mass cosmology in General Relativity. *Astron. Astrophys.*, 651:L13, 2021.

[45] Giovanni Manfredi, Jean-Louis Rouet, and Bruce Miller. The Bondi universe: How negative mass drives the cosmological expansion, 1 2026.

[46] Shin'ichi Nojiri and S. D. Odintsov. May Negative Mass Objects exist in the sky?, 2 2026.

[47] Andronikos Paliathanasis. Indications of a Late-Time Transition to a Strongly Interacting Dark Sector, 1 2026.

[48] Sean M. Carroll, Mark Hoffman, and Mark Trodden. Can the dark energy equation of state parameter w be less than -1? *Phys. Rev. D*, 68:023509, 2003.

[49] Prado Martin-Moruno and Matt Visser. Classical and semi-classical energy conditions. *Fundam. Theor. Phys.*, 189:193–213, 2017.

[50] Martin Kunz. The dark degeneracy: On the number and nature of dark components. *Phys. Rev. D*, 80:123001, 2009.

[51] R. F. vom Marttens, L. Casarini, W. Zimdahl, W. S. Hipólito-Ricaldi, and D. F. Mota. Does a generalized Chaplygin gas correctly describe the cosmological dark sector? *Phys. Dark Univ.*, 15:114–124, 2017.

[52] Rodrigo von Marttens, Lucas Lombriser, Martin Kunz, Valerio Marra, Luciano Casarini, and Jailson Alcaniz. Dark degeneracy I: Dynamical or interacting dark energy? *Phys. Dark Univ.*, 28:100490, 2020.

[53] Changyu You, Rong-Gen Cai, and Tao Yang. Breaking the Dark Sector Degeneracy with Nonparametric Expansion–Growth Reconstruction, 7 2026.

[54] Raphaël Kou and Antony Lewis. Unified dark fluid with null sound speed as an alternative to phantom dark energy. *JCAP*, 01:014, 2026.

[55] Yun-He Li and Xin Zhang. Large-scale stable interacting dark energy model: Cosmological perturbations and observational constraints. *Phys. Rev. D*, 89(8):083009, 2014.

[56] B. Wang, E. Abdalla, F. Atrio-Barandela, and D. Pavon. Dark Matter and Dark Energy Interactions: Theoretical Challenges, Cosmological Implications and Observational Signatures. *Rept. Prog. Phys.*, 79(9):096901, 2016.

[57] B Wang, E Abdalla, F Atrio-Barandela, and D Pavón. Further understanding the interaction between dark energy and dark matter: current status and future directions, 2024.

[58] Salvatore Capozziello, Himanshu Chaudhary, Tiberiu Harko, and Ghulam Mustafa. Is dark energy dynamical in the DESI era? A critical review. *Phys. Dark Univ.*, 51:102196, 2026.

[59] Timothy Clifton, Pedro G. Ferreira, Antonio Padilla, and Constantinos Skordis. Modified Gravity and Cosmology. *Phys. Rept.*, 513:1–189, 2012.

[60] Xin Zhang, Feng-Quan Wu, and Jingfei Zhang. New generalized chaplygin gas as a scheme for unification of dark energy and dark matter. *Journal of Cosmology and Astroparticle Physics*, 2006(01):003–003, January 2006.

[61] Yuting Wang, David Wands, Lixin Xu, Josue De-Santiago, and Alireza Hojjati. Cosmological constraints on a decomposed chaplygin gas. *Physical Review D*, 87(8), April 2013.

[62] Yun-He Li, Jing-Fei Zhang, and Xin Zhang. Parametrized post-Friedmann framework for interacting dark energy. *Physical Review D*, 90(6), September 2014.

[63] Ujjaini Alam, Varun Sahni, Tarun Deep Saini, and A. A. Starobinsky. Exploring the expanding universe and dark energy using the statefinder diagnostic. *Monthly Notices of the Royal Astronomical Society*, 344(4):1057–1074, October 2003.

[64] M. C. Bento, O. Bertolami, and A. A. Sen. Generalized Chaplygin gas, accelerated expansion and dark energy matter unification. *Phys. Rev. D*, 66:043507, 2002.

[65] M. C. Bento, O. Bertolami, and A. A. Sen. Generalized Chaplygin gas model: Dark energy - dark matter unification and CMBR constraints. *Gen. Rel. Grav.*, 35:2063–2069, 2003.

[66] Zong-Hong Zhu. Generalized Chaplygin gas as a unified scenario of dark matter/energy: Observational constraints. *Astron. Astrophys.*, 423:421–426, 2004.

[67] A. A. Sen and Robert J. Scherrer. Generalizing the generalized Chaplygin gas. *Phys. Rev. D*, 72:063511, 2005.

[68] Hachemi Benaoum. Accelerated Universe from Modified Chaplygin Gas and Tachyonic Fluid. *Universe*, 8(7):340, 2022.

[69] Ujjal Debnath, Asit Banerjee, and Subenoy Chakraborty. Role of modified Chaplygin gas in accelerated universe. *Class. Quant. Grav.*, 21:5609–5618, 2004.

[70] Chattree Wongsangwal, Khamphee Karwan, Stharporn Sapa, and Teeraparb Chantavat. Cluster number counts in dark energy model with energy and momentum coupling to dark matter, 1 2026.

[71] Havard Sandvik, Max Tegmark, Matias Zaldarriaga, and Ioav Waga. The end of unified dark matter? *Phys. Rev. D*, 69:123524, 2004.

[72] Yun-He Li, Jing-Fei Zhang, and Xin Zhang. Exploring the full parameter space for an interacting dark energy model with recent observations including redshift-space distortions: Application of the parametrized post-Friedmann approach. *Physical Review D*, 90(12), December 2014.

[73] Yun-He Li and Xin Zhang. IDECAMB: an implementation of interacting dark energy cosmology in CAMB. *Journal of Cosmology and Astroparticle Physics*, 2023(09):046, September 2023.

[74] Bilal Tüdes and Luca Amendola. Non-linear cosmological perturbations for coupled dark energy. *JCAP*, 09:001, 2025.

[75] Emanuelly Silva, Ubaldo Zúñiga-Bolaño, Rafael C. Nunes, and Eleonora Di Valentino. Non-linear matter power spectrum modeling in interacting dark energy cosmologies. *Eur. Phys. J. C*, 84(10):1104, 2024.

[76] Matheus Wolney, Gabriel Sampaio, Humberto Borges, Iuri Baranov, and Rodrigo von Marttens. Standard Perturbation Theory for Interacting Dark Sector cosmologies I: Breakdown of Einstein de Sitter kernels, 3 2026.

[77] Yuejia Zhai, Carsten van de Bruck, Eleonora Di Valentino, Baojiu Li, and Rafael C. Nunes. Non-linear Structure Formation in Planck+DESI Favoured Interacting Dark Energy Cosmologies, 6 2026.

[78] A. A. Escobal, H. A. P. Macedo, J. F. Jesus, R. C. Nunes, and J. A. S. Lima. Linear growth of matter perturbations probed by redshift-space distortions in interacting Λ(t)CDM cosmologies. *Phys. Dark Univ.*, 52:102320, 2026.

[79] Marcel van der Westhuizen and Amare Abebe. Crunching, bouncing, and cyclical cosmologies from dark sector interactions. *Classical and Quantum Gravity*, 2026. Accepted manuscript online 30 June 2026.